

Phase noise mitigation of QPSK signal utilizing phase-locked multiplexing of signal harmonics and amplitude saturation

Amirhossein Mohajerin-Ariaei,^{1,*} Morteza Ziyadi,¹ Mohammad Reza Chitgarha,¹ Ahmed Almainan,¹ Yinwen Cao,¹ Bishara Shamee,¹ Jeng-Yuan Yang,² Youichi Akasaka,² Motoyoshi Sekiya,² Shigehiro Takasaka,³ Ryuichi Sugizaki,³ Joseph D. Touch,⁴ Moshe Tur,⁵ Carsten Langrock,⁶ Martin M. Fejer,⁶ and Alan E. Willner¹

¹Department of Electrical Engineering, University of Southern California, Los Angeles, California 90089, USA

²Fujitsu Laboratories of America, 2801 Telecom Parkway, Richardson, TX 75082, USA

³Fitel Photonics Laboratories, Furukawa Electric Co., 6 Yawatakaigan-dori, Ichihara, Chiba, Japan

⁴Information Sciences Institute, University of Southern California, 4676 Admiralty Way, Marina del Rey, CA, 90292, USA

⁵School of Electrical Engineering, Tel Aviv University, Ramat Aviv 69978, Israel

⁶Edward L. Ginzton Laboratory, Stanford University, Stanford, California 94305, USA

*Corresponding author: mohajera@usc.edu

Received Month X, XXXX; revised Month X, XXXX; accepted Month X, XXXX; posted Month X, XXXX (Doc. ID XXXXXX); published Month X, XXXX

We demonstrate an all-optical phase noise mitigation scheme based on the generation, delay, and coherent summation of higher-order signal harmonics. The signal, its third-order harmonic, and their corresponding delayed variant conjugates create a staircase phase transfer function that quantizes the phase of QPSK signal to mitigate phase noise. The signal and the harmonics are automatically phase-locked multiplexed, avoiding the need for phase-based feedback loop and injection locking to maintain coherency. The residual phase noise converts to amplitude noise in the quantizer stage, which is suppressed by parametric amplification in the saturation regime. Phase noise reduction of ~40% and OSNR-gain of ~3dB at BER 10^{-3} are experimentally demonstrated for 20 and 30 Gbaud QPSK input signals. ©2015 Optical Society of America

OCIS Codes: (060.2360) Fiber optics links and subsystems; (060.4370) Nonlinear optics, fibers.

Advanced modulation formats such as quadrature-phase-shift-keying (QPSK) are gaining importance in high capacity optical networks [1,2]. In QPSK systems, phase or amplitude noise can cause a degradation in the received data's signal-to-noise ratio, resulting in a system power penalty. In specific, phase noise originating from interaction of ASE noise and Kerr nonlinearity can pose a key limitation in such systems [3,4].

Nonlinear phase noise of a high data rate signal can be reduced by taking advantage of electronic-based parallel data-processing techniques [2,5,6]. However, there might be advantages to mitigate the phase noise in the optical domain, such as avoiding the impact of optical-to-electronic conversion and supporting in-line signal processing for high baud rate signal [6]. Different approaches have been demonstrated for optical regeneration of QPSK signals using different variations of phase-sensitive-amplification to achieve a level of "phase squeezing" [7-9]. However, these methods tend to require coherency between a signal and a pump, typically requiring phase-based feedback loops and injection locking lasers [7-10].

Here, we propose and experimentally demonstrate a baud-rate-tunable phase noise mitigation scheme based on the generation, delay, and coherent summation of higher-order signal harmonics. Phase noise is mitigated in an all-optical phase quantizer by combining the signal, the conjugate copy and their delayed variant third harmonics. In the proposed method, the signal and the harmonics are automatically phase-locked multiplexed, avoiding the need for phase-based feedback loops and injection locking to maintain the coherency between different components of the quantization process [11].

Phase noise might be partially converted to amplitude noise in the quantizer stage [7,11]. Such converted

amplitude noise can be compensated, by means of an amplitude limiter. Therefore, a combined phase/amplitude noise mitigator can further improve the system performance.

The conceptual block diagram of the proposed approach is shown in Fig. 1. A QPSK signal contaminated with phase noise is coupled with a CW pump, and injected into a nonlinear wave mixer to generate a phase conjugate copy of the signal [12]. A nonlinear element with either second or third-order nonlinear susceptibility, $\chi^{(2)}$ or $\chi^{(3)}$, can be used in this stage to generate the copy. The signal and the conjugate copy are then sent into a $\chi^{(3)}$ medium to generate the third-order harmonics of the signal and the conjugate copy. In fact, these two stages can be combined in one stage by using a $\chi^{(3)}$ element with high amount of nonlinear efficiency [13]. The signal, its third-order harmonic, and their conjugates are sent into an optical programmable filter to apply appropriate delays and adjust amplitudes and relative phases. The adjusted signals and harmonics with a CW pump are injected into a $\chi^{(2)}$ medium to create a staircase phase transfer function. In this stage, the product of the signal and its delayed conjugate, and the product of the delayed third-order signal harmonic and the conjugate third-order harmonic are phase-locked multiplexed. This nonlinear process builds a staircase phase transfer function of the input signal, which results in squeezing the phase noise of the input signal. The residual phase noise which is not squeezed in the phase quantization process converts to amplitude noise due to the non-uniform amplitude profile of the staircase phase transfer function [7]. The amplitude noise is suppressed by utilizing an optical parametric amplifier operated in the saturation regime. If needed, the output signal can be wavelength converted back to the input signal wavelength

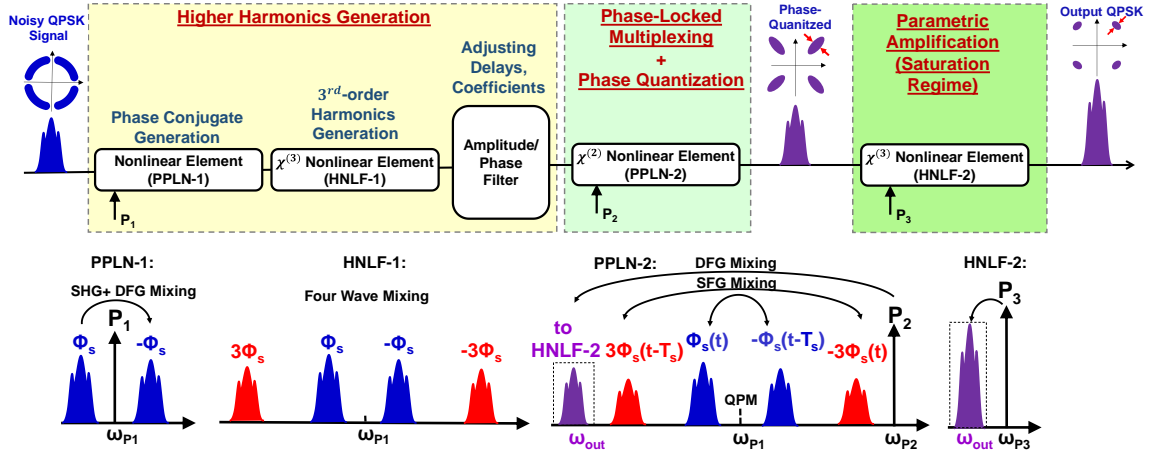


Fig. 1. The conceptual block diagram of the phase noise mitigation scheme.

using common all-optical wavelength conversion methods.

In the following, the mathematical descriptions of nonlinear stages to create the phase quantization function are presented.

A periodically-poled lithium niobate (PPLN) waveguide is used in the first nonlinear stage. The wavelength of the first pump laser $P_1(t)$ is set to the quasi-phase matching (QPM) wavelength of PPLN-1. This pump interacts with itself through a second-harmonic-generation process, and creates the mixing term $P_1^2(t)$ at $2\omega_{p1}$. The SHG term then mixes with the input signal $S_{in}(t)$ through the difference-frequency-generation (DFG) process to create a phase conjugate replica at $2\omega_{p1} - \omega_{in}$ with the electric field proportional to $P_1^2(t) \times S_{in}^*(t)$. The PPLN-1 output is sent into an in-line spatial light modulator (SLM) to filter out the pump. The signal and its conjugate are mixed through a four-wave-mixing (FWM) process in a highly nonlinear fiber (HNLF) to generate the third-order harmonics at $-2\omega_{p1} + 3\omega_{in}$ and $4\omega_{p1} - 3\omega_{in}$. The electric field of the generated third-order harmonics are proportional to $P_1^2(t) \times S_{in}^3(t)$ and $P_1^4(t) \times S_{in}^3(t)$. In a liquid crystal on silicon (LCoS) programmable filter, one symbol delay (T_s) is applied between: (i) the signal and its conjugate copy, and (ii) the generated third-order harmonics. In addition, amplitudes and relative phases are adjusted in the LCoS. In the second PPLN waveguide, the signal and its delayed conjugate are mixed through a sum-frequency-generation (SFG) nonlinear process and generate a new signal at $2\omega_{p1}$ with the electric field of $E_1(t)$ proportional to

$$E_1(t) \propto P_1^2(t - T_s) \times [S_{in}(t) \times S_{in}^*(t - T_s)] \quad (1)$$

Similarly, in a parallel process, the third-order harmonics are mixed through an SFG process and generate a new signal at $2\omega_{p1}$ with the electric field of $E_2(t)$ proportional to

$$E_2(t) \propto P_1^2(t - T_s) \times P_1^4(t) \times [S_{in}(t - T_s) \times S_{in}^*(t)]^3 \quad (2)$$

The challenge of combining the signals $E_1(t)$ and $E_2(t)$ at $2\omega_{p1}$ result from the fact that they need to be phase locked and have the same phase reference. According to Eqs. (1) and (2) the phases of $E_1(t)$ and $E_2(t)$ can be expressed as:

$$\Phi_{E1}(t) = 2\Phi_{P1}(t - T_s) + \Delta\Phi_{in}(t) \quad (3)$$

$$\begin{aligned} \Phi_{E2}(t) &= -2\Phi_{P1}(t - T_s) + 4\Phi_{P1}(t) - 3\Delta\Phi_{in}(t) \\ &= 2\Phi_{P1}(t - T_s) + 4\Delta\Phi_{P1}(t) - 3\Delta\Phi_{in}(t) \end{aligned} \quad (4)$$

where $\Phi_{in}(t)$ and $\Phi_{P1}(t)$ refer to the phase of the input signal and the pump, respectively. Moreover, Δ is defined as a difference operator for one symbol interval T_s , i.e., $\Delta\Phi(t) \triangleq \Phi(t) - \Phi(t - T_s)$. In order to study the

coherence of $E_1(t)$ and $E_2(t)$, the phase noise of the input signal, $\Phi_{in}^N(t)$, and the phase noise of the pump, $\Phi_{P1}^N(t)$, need to be considered in Eqs. (3) and (4), except for the first similar term $2\Phi_{P1}(t - T_s)$.

$$\Phi_{E1}(t) = 2\Phi_{P1}(t - T_s) + \Delta\Phi_{in}^D(t) + \Delta\Phi_{in}^N(t) \quad (5)$$

where $\Phi_{in}^D(t)$ refers to the QPSK data and $\Delta\Phi_{in}^D(t) = \Phi_{in}^D(t) - \Phi_{in}^D(t - T_s)$ represents the simple encoded version of the original signal and has the same format as differential phase shift keying modulation. Eq. (6) uses the fact that for QPSK data $\exp(-j3\Phi_{in}^D(t)) = \exp(j\Phi_{in}^D(t))$; and the term $-3\Delta\Phi_{in}^D(t)$ is replaced by $\Delta\Phi_{in}^D(t)$.

Assuming that the phase noise of the pump, $\Phi_{P1}^N(t)$, is from the laser linewidth ($\Delta\nu$), and its fluctuation is significantly slower than the symbol rate ($\Delta\nu \ll 1/T_s$), we conclude that $\Delta\Phi_{P1}^N(t) = \Phi_{P1}^N(t) - \Phi_{P1}^N(t - T_s)$ is negligible. By performing Fourier transform of $\Delta\Phi_{P1}^N(t)$, the result is:

$$\mathcal{F}(\Delta\Phi_{P1}^N(t)) \triangleq 2j \exp(-j\omega T_s/2) \sin(\omega T_s/2) \times \Phi_{P1}^N(\omega) \quad (7)$$

Because the power spectral density (PSD) of the differentiator, $|\sin(\omega T_s/2)|^2$, rejects the lower frequency components of $\Phi_{P1}^N(\omega)$ (as shown in Fig. 2), the PSD of the $\Delta\Phi_{P1}^N(t)$ contains almost no power assuming $\Delta\nu \ll 1/T_s$.

A CW pump with an electric field of $P_2(t)$ is injected into the PPLN-2 waveguide to convert the SFG signal at $2\omega_{p1}$ to the new signal $S_{out}(t)$. The electric field of $S_{out}(t)$ is proportional to:

$$S_{out}(t) \propto e^{j2\Phi_{P1}(t)} e^{j\Delta\Phi_{in}^D(t)} \left[e^{j\Delta\Phi_{in}^N(t)} + m e^{-j3\Delta\Phi_{in}^N(t)} \right] \quad (8)$$

where the value of m is defined as $m \triangleq |E_2|/|E_1|$, and can be adjusted in the LCoS filter [7]. The term inside the brackets in Eq. (8) enables the function of squeezing the phase noise of the input signal. If the value of m in the squeezing function is set to zero by bypassing the higher harmonics generation stage in Fig. 1, the term inside the brackets in Eq. (8) is simplified to $\exp(j\Delta\Phi_{in}^N(t))$. This function is a differentiator on the phase domain and is able to mitigate phase noise with low-bandwidth PSD, such as phase noise coming from laser linewidth [12].

Figure 3(a) shows the experimental setup for verifying the phase noise mitigation scheme. 20/30-Gbaud QPSK data (PRBS 2³¹-1) is generated using a CW laser at 1550 nm. The signal is phase modulated with an ASE source followed by a variable optical attenuator (VOA) and a photo-diode (PD) to induce phase noise with different power levels. The noisy signal is amplified to 23 dBm and

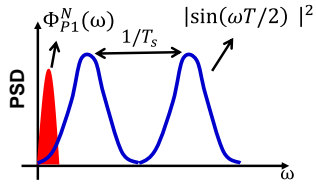


Fig. 2. The PSD of the phase-differentiator.

coupled with a 26 dBm amplified CW pump around 1551.5nm and injected into PPLN-1 waveguide. A ~450m HNL-1 (ZDW at 1551.5nm) is used to generate the third-order harmonics. A 23 dBm amplified CW pump at 1543nm is injected into the PPLN-2 waveguide to multiplex the signals. The generated signal is amplified to ~10 dBm and coupled with a 30 dBm amplified CW pump, around 1556.3nm, and injected into a 700m dispersion stable HNL-2 (ZDW at 1551.5 nm). The pump is phase modulated with 4.5 GHz PRBS ($2^{15}-1$) data to suppress stimulated Brillouin scattering. Figure 3(c) shows the measured gain and output power profiles of HNL-2. Finally, the output signal is captured by a coherent detector, without applying DSP equalization, to measure the phase noise range, EVM, and BER.

The system performance is assessed using 20 and 30-Gbaud QPSK signals. Figure 4 shows the constellation diagrams of the 20-Gbaud input noisy signal and the output of the phase quantizer. The results are obtained for different values of phase noise. In order to compare the phase noise range between the constellation diagrams, the parameter $\delta\phi$ is defined to quantify the phase deviation from the corresponding expected value, showing the standard deviation of the phase. In addition, the parameter $\delta\rho$ is defined as the percentage of amplitude deviation from the expected value, showing the relative standard deviation of the amplitude. As can be seen in Fig. 4, phase noise is reduced by phase quantizer, in particular for higher levels of noise. In Fig. 4(a), $\delta\phi$ is reduced by ~49%. The value of $\delta\rho$ is, however, increased by ~56%. This indicates that phase noise is partially converted to amplitude noise in the phase quantizer. The amplitude noise can be suppressed by utilizing a parametric amplification in the saturation regime. Figure 5 shows the constellation diagrams of 30-Gbaud noisy QPSK signals,

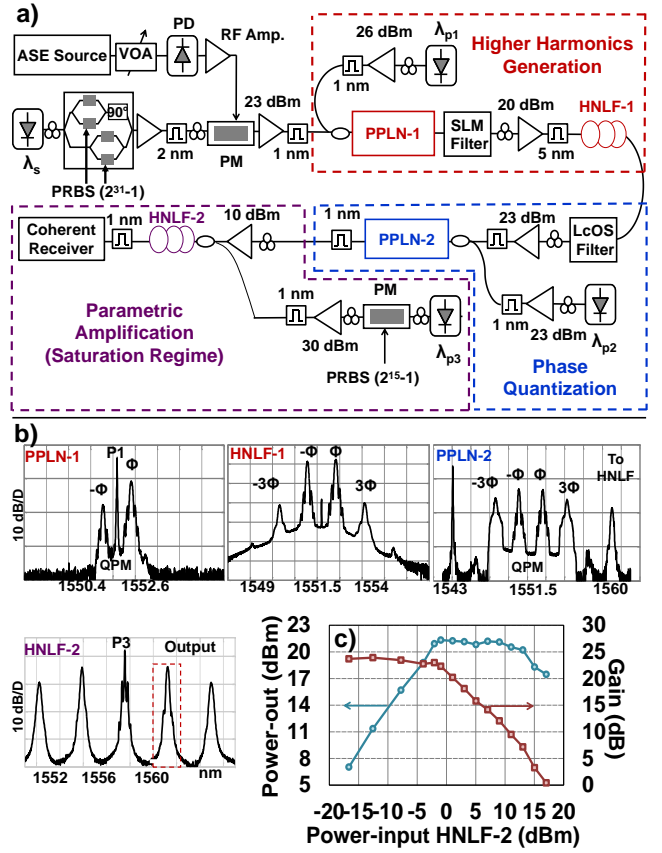


Fig. 3. (a) Experimental setup of the phase noise mitigation scheme. (b) Spectra of the output of the nonlinear stages. (c) Power and gain profiles of HNL-2.

and the corresponding outputs of the phase quantizer, and the parametric amplifier. As can be seen, phase noise and amplitude noise are decreased in the output of parametric amplifier. In Fig. 5(a), $\delta\phi$ is reduced by ~40%, and $\delta\rho$ is reduced by 16% in the output of parametric amplifier compared to the input signal. As a result, the EVM between the input signal and the final output is decreased by ~36% in Fig. 5(a). Figure 6(a) shows the percentage of phase noise reduction for 30-Gbaud input noisy QPSK signal, in the output of phase noise quantizer and the

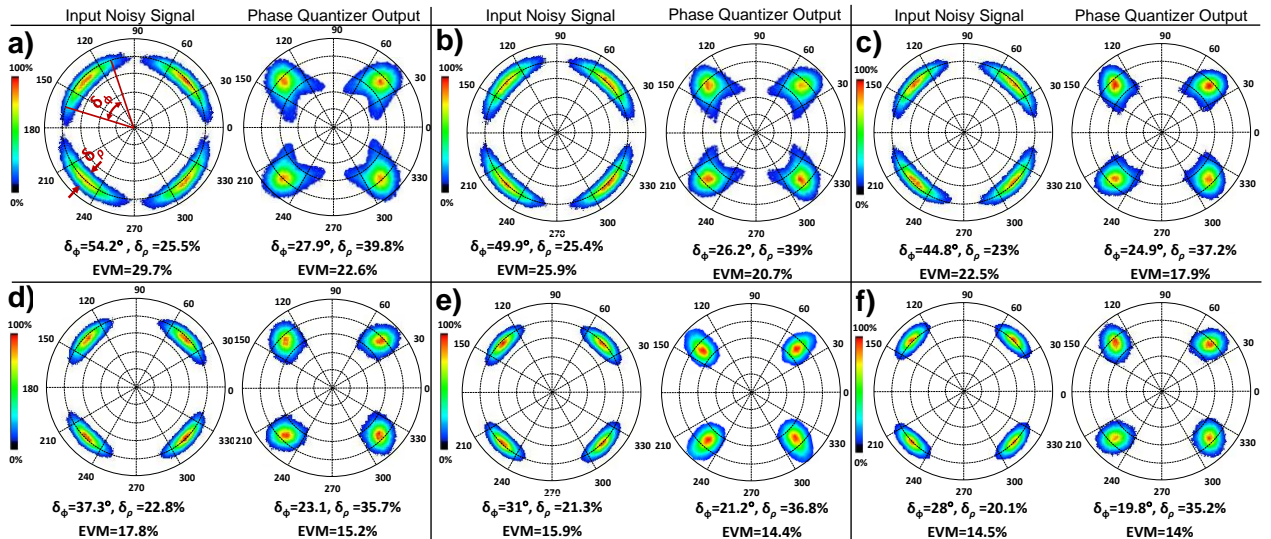


Fig. 4. The constellation diagrams of the input and output of phase quantizer for different levels of phase noise.

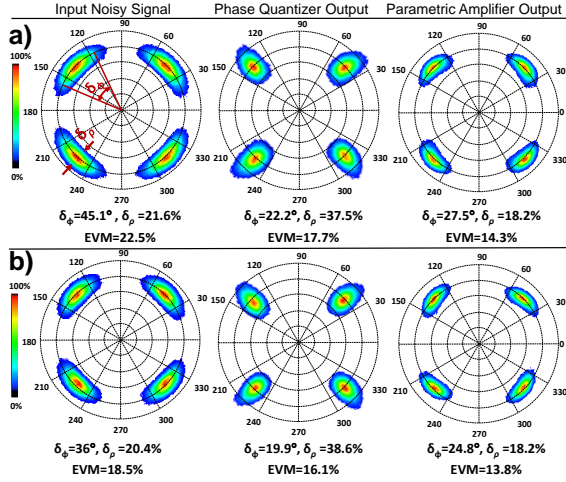


Fig. 5. The constellation diagrams of 30-Gbaud QPSK signal, and the outputs of the phase quantizer and parametric amplifier for two noise levels.

output of parametric amplifier. The amount of reduction is increased for higher levels of phase noise and it becomes gradually constant for the phase noise with $\delta\phi > 50^\circ$. Moreover, the amount of phase noise reduction in the parametric amplifier output is less than the amount of reduction in the phase quantizer output. This fact indicates that the amplitude saturation stage adds some phase noise to the output of the phase quantizer. Figure 6(b) shows the EVMs of the 30-Gbaud input noisy QPSK signal, and the corresponding outputs of the phase quantizer and the parametric amplifier for various levels of phase noise. The EVM is improved in the system output (parametric amplifier output), and remained between 13% to 18% for different levels of phase noise.

Figure 7 shows the BER curves of the phase noise mitigation scheme for two different levels of phase noise, $\delta\phi \sim 43^\circ$ and $\sim 35^\circ$. Near 1.5 dB OSNR gain is achieved in the

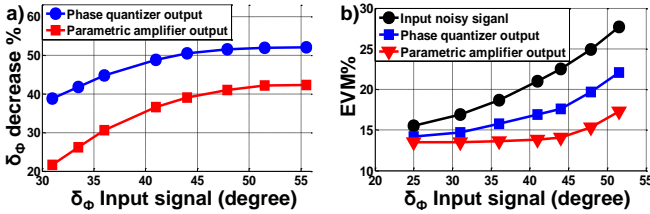


Fig. 6. (a) Percentage of phase noise range reduction for various levels of phase noise for 30 Gbaud QPSK signal. (b) EVM of the input noisy signal, phase quantizer output, and parametric amplifier output for various levels of phase noise for 30 Gbaud QPSK signal.

phase quantizer output at BER of 10^{-3} . By suppressing the amplitude noise in the parametric amplifier, near 3 dB OSNR gain is achieved at BER 10^{-3} .

An all-optical nonlinear phase noise mitigation is demonstrated based on the phase-locked multiplexing of signal harmonics and amplitude saturation, avoiding the need for phase-based feedback loops and injection locking. The phase locking process converts the signal format to differential phase shift keying. Further studies are needed to investigate a phase-locked method without format conversion. Moreover, in this letter, we focused on the QPSK signal contaminated only with phase noise. For the signal with amplitude noise, it might be possible to

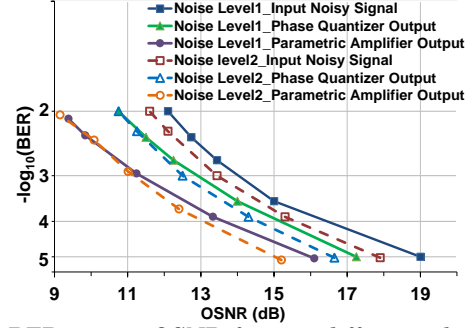


Fig. 7. BER versus OSNR for two different phase noise levels ($\delta\phi \sim 43^\circ, \sim 35^\circ$).

suppress the amplitude noise in an extra nonlinear stage using the amplitude saturation method, and then mitigate the remained phase noise by utilizing the proposed phase noise mitigation method.

This work was supported by the NSF and CIAN.

References

1. P. J. Winzer, *IEEE Commun. Mag.* **48**, 26 (2010).
2. E. Ip, A. P. T. Lau, D. J. F. Barros, and J. M. Kahn, *Opt. Express* **16**, 753 (2008).
3. J. P. Gordon and L. F. Mollenauer, *Opt. Lett.* **15**, 1351 (1990).
4. A. Demir, *J. Lightwave Technol.* **25**, 2002 (2007).
5. X. Li, X. Chen, G. Goldfarb, E. Mateo, I. Kim, F. Yaman, and G. Li, *Opt. Express* **16**, 880 (2008).
6. R. Slavík, F. Parmigiani, J. Kakande, C. Lundström, M. Sjödin, P. A. Andrekson, R. Weerasuriya, S. Sygletos, A. D. Ellis, L. Grüner-Nielsen, D. Jakobsen, S. Herström, R. Phelan, J. O'Gorman, A. Bogris, D. Syvridis, S. Dasgupta, P. Petropoulos & D. J. Richardson, *Nat. Photonics* **4** (2010).
7. J. Kakande, R. Slavík, F. Parmigiani, A. Bogris, D. Syvridis, L. Grüner-Nielsen, R. Phelan, P. Petropoulos, and D. J. Richardson, *Nat. Photon.* **5**, 748 (2011).
8. T. Umeki, M. Asobe, H. Takara, Y. Miyamoto, & H. Takenouchi, *Opt. Express* **21**, 12077 (2013).
9. K. Solis-Trapala, J. Kurumida, M. Gao, T. Inoue, and S. Namiki, *PTL* **26**, 629 (2014).
10. M. Asobe, T. Umeki, H. Takenouchi, and Miyamoto, *Opt. Express* **22**, 26642 (2014).
11. A. Mohajerin-Ariaei, Y. Akasaka, J.-Y. Yang, M. R. Chitgarha, M. Ziyadi, Y. Cao, A. Almainan, J. D. Touch, M. Tur, M. Sekiya, S. Takasaka, R. Sugizaki, C. Langrock, M. M. Fejer, and A. E. Willner, in *European Conference on Optical Communication (ECOC)*, paper P.3.20 (2014).
12. M. R. Chitgarha, S. Khaleghi, M. Ziyadi, A. Mohajerin-Ariaei, A. Almainan, W. Daab, D. Rogawski, M. Tur, J. D. Touch, C. Langrock, M. M. Fejer, and A. E. Willner, *Opt. Letters* **39**, 2928 (2014).
13. J. Kakande, A. Bogris, R. Slavík, F. Parmigiani, D. Syvridis, P. Petropoulos, and D. J. Richardson, in *Proc. of European Conference on Optical Communications (ECOC)*, post deadline PD 3.3.